JOURNAL OF CATALYSIS **170,** 37–45 (1997)
ARTICLE NO. CA971733

Characterization of Acid–Base Paired Sites on Silica-Supported RuS_2 by Infrared Spectroscopy and Methyl Mercaptan Condensation Reaction

Gilles Berhault,* Michel Lacroix,* Michèle Breysse,*,[1] Françoise Maugé,† Jean-Claude Lavalley,† and Lianglong Qu‡

*Institut de Recherches sur la Catalyse, 2, Avenue Albert Einstein, 69626 Villeurbanne Cedex, France; †Laboratoire Catalyse et Spectrochimie, ISMRA-Université, 6, Boulevard du Maréchal Juin, 14050 Caen Cedex, France; and ‡Research Institute of Petroleum Processing, 18 Xueyuan Road, P.O. Box 914, Beijing 100083, China

Received February 12, 1997; revised April 8, 1997; accepted April 11, 1997

The aim of this work was to find out a simple test reaction allowing the characterization of the acid–base properties of sulfided catalyst. This study was carried out using a silica-supported ruthenium sulfide phase as model catalyst and the condensation of methylthiol as test reaction. The choice of the RuS_2 phase was dictated by its ability to lose an important amount of sulfur without changing its morphological and structural properties. The use of several techniques such as temperature-programmed reduction, high resolution electron microscopy, and X-ray diffraction have evidenced that about 45% of the initial sulfur content may be removed upon reduction while maintaining the pyrite structure. This reductive treatment modifies the concentration of coordinatively unsaturated sites and that of the surface sulfur species inducing by the way a change in the number of acid–base centers. The characterization of the interaction of CH_3SH with these reduced states by Fourier transform infrared spectroscopy has demonstrated that this probe dissociates upon chemisorption leading to the formation of a proton and to a thiolate type moiety. This heterolytic character of the adsorption implies the presence of both a Lewis acidic type site to fix the organic fragment and the presence of a basic sulfur center to trap the positively charged hydrogen species. The combination of quantitative IR data with catalytic activity measurements has evidenced that the thioether formation is directly related to the concentration of thiolate species indicating that they are probably a reaction intermediate. It is thus concluded that the methyl mercaptan condensation reaction would give pertinent information on the acid–base properties of sulfide catalysts.

INTRODUCTION

Sulfides find extensive use as hydrotreating catalysts. Hydrotreating refers to several reactions that include hydrogenation and carbon–heteroatom hydrogenolysis reactions such as hydrodesulfurization and hydrogenation. In order to catalyze simultaneously all these reactions, sulfide catalysts operate at temperatures ranging between 573 and 673 K in the presence of a large excess of hydrogen (1). In the past two decades, extensive work devoted to the understanding of these materials has evidenced that their catalytic properties are related to the presence of coordinatively unsaturated sites (CUS) created by sulfur removal of the catalyst surface under the reductive atmosphere required to carry out the catalytic process (2–5). On such sulfur vacant sites chemisorption of unsaturated hydrocarbons proceeds by π-electron donation while bonding of sulfur- and nitrogen-containing molecules may also occur via the lone pair of electrons present on the heteroatom to be removed by hydrogenolysis (2, 6, 7). Therefore, CUS intervene as electron-withdrawing sites which properties may be regarded as a Lewis type center interacting with electron-donating organic substrates. Besides these vacancy sites, the existence of sulfhydryl groups has been observed by several techniques such as inelastic neutron scattering (8–12), ^{1}H NMR (13, 14), and Raman and Fourier transform infrared (FTIR) spectroscopy (15, 16). While there is a general agreement in the literature concerning the importance of CUS for developing catalytic properties in all reactions involved in the hydrotreatment, many studies related to the determination of model reaction mechanisms have also assumed that the presence of SH groups could be of prime importance (17–22). The formation of such SH entities may arise either from the heterolytic adsorption of H_2 on both a surface vacancy and a neighbor sulfur atom or by heterolytic chemisorption of H_2S which is almost always present in the feed during the determination of the catalytic activity. Accordingly, the surface of a sulfide catalyst possesses Lewis sites (CUS), SH groups, and obviously sulfur anions, their amount being dependent on the temperature and also on the composition of the surrounding atmosphere.

Acidity and basicity are paired concepts which are very often invoked to explain the catalytic properties of oxides. In this field, many IR studies have been devoted to acidity determination because of the importance of acidic materials

[1] Present address: Laboratoire de Réactivité de Surface, Université P. et M. Curie, 4, place Jussieu, Casier 178, 75252 Paris Cedex 05, France.

0021-9517/97 $25.00

for petroleum chemistry (23–26) while much less attention has been paid to the characterization of acid–base pairs as well as basicity. The use of probes which could dissociatively chemisorbed at the surface of the catalyst was proposed for the titration of acid–base centers. For instance, hydrogen was used for the titration of the acid–base centers of ZnO surface (27). Alcohols were recognized to dissociate on the surface of oxides (28, 29). Their chemisorptions lead to the formation of alkoxy groups and the resulting proton further interacts with a basic oxygen giving rise to an increase of the concentration of hydroxyl species. This suggests that the presence of acid–base pairs is a necessary prerequisite for alcohols chemisorption. These data were mostly evidenced at room temperature using FTIR spectroscopy while at higher temperature alcohols easily undergo a condensation reaction leading to the formation of ethers (30–33). But as the first step of ether formation requires the chemisorption of the reactant, this reaction might be regarded as a fingerprint of the acid–base properties of the solid. The transposition of this methodology to sulfide catalysts is not straightforward. For example, hydrogen cannot be utilized for the IR characterizations of sulfide catalysts because the nature of its chemisorption is still not completely elucidated and because the resulting SH group leads to weak IR bands. The same reason impedes of course the use of H_2S. Consequently, it appeared profitable to us to find out a simple reaction which may account for the acid–base properties of a sulfided phase. If this reaction exists its advantage would be to characterize the properties of a given sulfide under experimental conditions close to the ones employed in hydrotreating, i.e., high temperature, high hydrogen pressure, and role of H_2S on solid properties. According to Mashkina *et al.* (34) chemisorption of alcohols or of thiols proceeds on similar sites of solid oxide surfaces. By analogy to this work, we have preferred to study the disproportionation of thiols into thioethers and H_2S instead of alcohol condensation in order to avoid the possible oxidation of the catalysts by such oxygen containing molecules. Moreover, the lightest thiol (CH_3SH) was used as reactant to exclude the dehydrogenation reaction leading to olefinic compounds. The characterization of chemisorbed species was carried out by means of FTIR.

In a first approach, a silica-supported ruthenium sulfide was used as model catalyst. The silica carrier was chosen in order to avoid any contribution of the support to the acidity of the system while the ruthenium sulfide phase was selected because of its high activity for performing hydrogenation and hydrodesulfurisation reactions (35, 36). Recently, it has been found that the unsupported RuS_2 phase was highly reducible since the sulfur to metal ratio may vary from 2.25 to 0 by treating the solid under hydrogen at temperatures as low as 723 K (5, 12, 14). Moreover, physicochemical characterizations have evidenced that upon reduction, about 45% of the initial sulfur content may be removed without changing the structural and morphological properties of the initial pyrite structure (5). Inelastic neutron scattering experiments and hydrogen thermodesorption measurements have shown that solid reduction modifies the number of vacant sites as well as the concentration of SH groups (12). Therefore, significant variations of the acid–base properties could be expected depending on the catalyst pretreatment. This behavior makes RuS_2 a suitable solid for characterizing variation of acid–base properties induced by a reduction of the solid.

EXPERIMENTAL

Catalyst Preparation

Silica-supported ruthenium sulfide was prepared using the pore filling method. The support is a Davison 432 silica of 300 m^2/g BET area having a pore volume of 0.5 cm^3/g which was dried overnight at 383 K prior to the impregnation. Aqueous solution of $RuCl_3 \cdot xH_2O$ (from Jonhson Matthey) was used as ruthenium salt precursor. After impregnation at room temperature for 3 h, the solid was dried at 383 K under vacuum before its transformation into a sulfided phase. This sulfidation step was performed by heating the precursor at 673 K with a 15% H_2S–85% N_2 atmosphere in order to avoid the intermediate formation of a metallic phase which is known to be difficult to sulfide (37). After this activation procedure, the solid was cooled to room temperature in the presence of the sulfur-containing atmosphere, flushed with an oxygen-free nitrogen flow, and stored in sealed bottles. The ruthenium content determined by chemical analysis was 7.5 wt% and the catalyst composition corresponded to $RuS_{2.7}$ with a residual chlorine content lower than 0.01%.

Electron Microscopy

High resolution electron microscopy (HREM) examinations were performed with a Jeol 100 CX instrument fitted with a UHP polar piece (resolving power, 0.2 nm). After the hydrogen treatment, the reduced solids were immediately immersed into deoxygenated heptane at room temperature in order to prevent their oxidation. Then the samples were ultrasonically dispersed in this solvent and the suspension was collected on a carbon coated copper grid. Particle size distribution was determined by counting about 500–600 particles. The average particle size was calculated according to the first moment of the distribution:

$$\frac{\sum_{i=1}^{n} n_i L_i}{\sum_{i=1}^{n} n_i}$$

X-Ray Diffraction

X-ray diffraction (XRD) measurements were performed to determine the structural stability and the modification

of the particle size of the various reduced solids. The XRD patterns were collected in the 2θ domain ranging from 5° to 80° using a Siemens D500 diffractometer using the Cu$K\alpha$ radiation source operating at 45 kV and 35 mA. The reduced solids were transferred to the sample holder in a glove box and an adhesive tape was used to protect them from air oxidation.

Catalyst Reduction

The *in situ* reduction of the catalyst was performed in a flow microreactor connected to a gas chromatograph (HP 5890A) equipped with a flame photometric detector (FPD) which allows the detection of sulfur-containing molecules. After loading the sample into the reactor, the solid was flushed under nitrogen for 15 min and then contacted with a hydrogen flow of 100 cm^3 min^{-1} at room temperature. The reactor was then heated up to the desired reduction temperature using a heating rate of 2 K min^{-1}. The amount of H_2S released by the solid during the reduction process was quantified by calibrating the detector with a known concentration of H_2S (1153 ppm) diluted in hydrogen. The degree of reduction was defined by the ratio of the amount of H_2S eliminated from the solid to the total sulfur content.

Catalytic Activity

After an *in situ* reduction, hydrogen was replaced by nitrogen and the reactor temperature was fixed at 473 K. The reduced catalyst was then submitted to a flow of MeSH/N_2 (63 cm^3 min^{-1}). The partial pressure of methyl mercaptan (MeSH) was 40 Torr. The analysis of the reaction mixture was performed with a HP 5890A gas chromatograph equipped with HP-5 capillary column (crosslinked Ph–Me Silicon, 50 m × 0.32 mm × 0.25 μm) maintained at 333 K. Besides the reactant (MeSH), only H_2S, and dimethyl sulfide (DMS) were detected under these experimental conditions. Their retention times are respectively 4.6, 4.3, and 5.5 min. As a FPD detector is extremely sensitive toward sulfur-containing molecules, it was used only to quantify the H_2S production while the hydrocarbons were analyzed using a FID detector. Conversions were kept lower than 10% by adjusting either the catalyst weight or the total flow in order to avoid possible mass transfer limitations.

FTIR Spectroscopy

FTIR characterization of adsorbed CH_3SH was performed using self-supporting discs (5 mg cm^{-2}) of pressed samples. As this pelletizing step cannot be done without air exposure, the catalysts were resulfided *in situ* in the infrared transmission cell. For this purpose, the pellet was first evacuated at room temperature and then contacted with 100 Torr of H_2S(15%)–He. The cell was then heated up to 673 K with a heating rate of 10 K min^{-1} and maintained at this temperature for 30 min. The sulfidation was followed by an evacuation at 673 K for 30 min. This sulfidation–evacuation procedure was repeated twice and the system was cooled to room temperature (RT) under evacuation before solid reduction. Then 200 Torr of pure hydrogen is introduced in the cell which is then heated up to the desired reduction temperature. Several reduction–evacuation cycles were performed in order to remove the H_2S formed upon reduction. At last, all the samples were evacuated at 393 K for 30 min prior to probe molecules adsorption. CH_3SH adsorptions were first performed at room temperature using 4 Torr of CH_3SH. Under these conditions, preliminary experiments have shown that adsorption reaches rapidly an equilibrium. The IR spectra were recorded using a Nicolet 60SX spectrometer either after evacuation of the gas phase at room temperature or at various temperatures in order to estimate the bond strength of the adsorbate with the solid surface. Band intensities were corrected from slight differences in catalyst weight and band areas were calculated by integration using the IR Omnic software.

RESULTS

Solid Reduction

The starting point of this work was to investigate how the silica-supported catalyst behaves toward a hydrogen atmosphere. Preliminary experiments have shown that the silica support sulfided under the same conditions does not release H_2S when submitted to a hydrogen flow from RT up to 1073 K. Figure 1 shows the evolution of the cumulated amount of H_2S released by the solid against time for various temperatures. In this set of experiments, the solid is first contacted with hydrogen at RT for 0.5 h and the system is

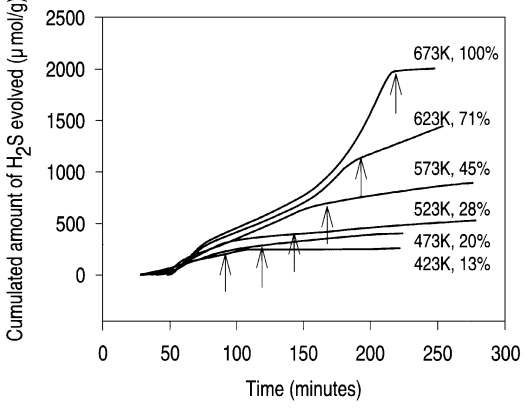

FIG. 1. Evolution of the cumulated amount of H_2S released by the catalysts in the presence of hydrogen at various temperatures. Experimental conditions: Hydrogen pressure, 760 Torr (1 Torr = 133.33 N m^{-2}); Hydrogen flow, 110 cm^3/min; heating rate, 2 K/min. The arrows indicate the time required to reach the reduction temperature and the percentages give the degree of reduction of the solid.

then heated up to the desired temperature (2 K min^{-1}) and left at this temperature for about 2 h. The arrows point for the time required to reach the temperature of reduction. For temperatures ranging from 423 to 573 K, the observed S-shaped curves indicate that H_2S is mostly produced during heating since its amount rapidly levels off when the reduction proceeds under isothermal conditions. This behavior shows that solid composition expeditiously equilibrates with the reducing atmosphere and suggests that the S/Ru ratio is mostly controlled by the temperature rather than by the time on stream. At 623 K, the solid continuously loses sulfur whatever the reduction time, and at 673 K, the sulfide phase is entirely reduced since the amount of sulfur removed corresponds to the one determined by chemical analysis (2000 μmol/g; S/Ru = 2.7).

Physicochemical Characterizations

HREM micrographs of the nonreduced or hydrogen reduced samples exhibit nearly spherical particle shapes dispersed at the surface of the support independently of the severity of the solid pretreatment. As shown in Fig. 2 the initial nonreduced solid presents a pretty homogeneous particle size distribution since more than 90% of the observed spheres have a size ranging between 25 and 45 Å. A reduction of the sample at either 473 or 573 K does not modify either the average particle size or the distribution width. Taking into account the amount of H_2S released at 573 K, it appears that about 45% of the initial sulfur content can be removed without any noticeable modification of the morphology of the sulfided phase. For higher reduction temperatures, the Ru-containing phase sinters and the distribution greatly enlarges as far as sulfur is further removed from the solid.

The XRD characterization of these solids is illustrated in Fig. 3. The large peak centered at $2\theta = 20^\circ$ and the shoulder at $2\theta = 9^\circ$ come from the silica support and the film used to protect the sample from air oxidation during the measurement. The nonreduced solid presents three other peaks located at $2\theta = 32$, 46, and 54, respectively, assigned to the [200], [220], and [311] faces of the RuS_2 pyrite phase. A hydrogen treatment performed up to 573 K does not modify either the position or the broadening of these diffraction lines. Thus the structure and the particle size of the solid appear to be stable and in fairly good agreement with the HREM results. At 623 K, the appearance of a new peak at $2\theta = 43^\circ$ corresponding to the [101] plane of the metallic phase indicates that the system becomes biphasic. At higher temperature of reduction, the diffraction lines of the sulfide phase have disappeared and only those corresponding to the metal were detected respectively at $2\theta \approx 38.5$ [100], 42.2 [002], 44 [101], 58.4 [102], and 69.5° [110]. This result is in agreement with the temperature-programmed reduction (TPR) ones.

CH_3SH Condensation Reaction

The catalytic properties of these reduced solids are illustrated in Fig. 4. Preliminary experiments have shown that the silica carrier is not active in this reaction. The specific activity was determined after only 6 h time on stream because the solids do not exhibit any significant deactivation. The filled square refers to the activity of the nonreduced solid. Its activity was determined by heating the catalyst up to the reaction temperature (473 K) in the presence of a nitrogen flow. During this step, only 0.1% of the initial sulfur content is released upon heating. This negligible amount of H_2S may result either from the desorption of weakly bonded species retained by the solid upon sulfiding or by reaction between two neighbor SH groups. As shown in Fig. 4, this solid possesses a significant activity. The progressive reduction of the catalyst leads to noticeable changes of the condensation rate. The activity increases first as far as sulfur is removed upon reduction, reaches a maximum for a degree of reduction of about 20%, and then gradually diminishes when the S to metal ratio tends to 0. The presence of an activity maximum suggests that this reaction may require an appropriate proportion of CUS, SH, or S^{2-} anions to proceed. The remaining activity of the completely reduced solid is not surprising because metals are known to react with alkane or arylthiols (38, 39).

CH_3SH Adsorption

The adsorption of CH_3SH on the silica carrier gives rise to four absorption bands located at 3012, 2948, 2858, and 2590 cm^{-1} (Fig. 5). By comparison with literature data the three high frequency bands are respectively ascribed to $\nu_a(CH_3)$, $\nu_s(CH_3)$, and $2\delta_a(CH_3)$ vibrations while the band at 2590 cm^{-1} corresponds to the ν(SH) stretching mode whose wavenumber is very close to that of the free molecule (40, 41). In parallel, a strong decrease of the intensity of the 3740 cm^{-1} band characterizing SiO–H stretching mode is observed and a broad band at 3475 cm^{-1} assigned to perturbed SiO–H vibrations appears. These data reflect a nondissociative adsorption of the probe molecule on silica suggesting that adsorption may occur by hydrogen bonding with some OH groups of the support. The presence of such weakly bonded species is consistent with the reversible character of the adsorption since all the bands vanished upon evacuation at RT. The silica-supported ruthenium sulfide exhibits a completely different behavior. The CH bands are drastically shifted toward lower wavenumbers indicating a nature of the adsorbed species different from those adsorbed on the support. Their intensities slightly decrease under vacuum and this species is still present on the catalyst even after an evacuation at 393 or 473 K. This behavior indicates that CH_3SH is strongly adsorbed at the surface of the sulfided phase. Furthermore, it should be underlined that on such a system, the ν(SH) vibration is no longer observed

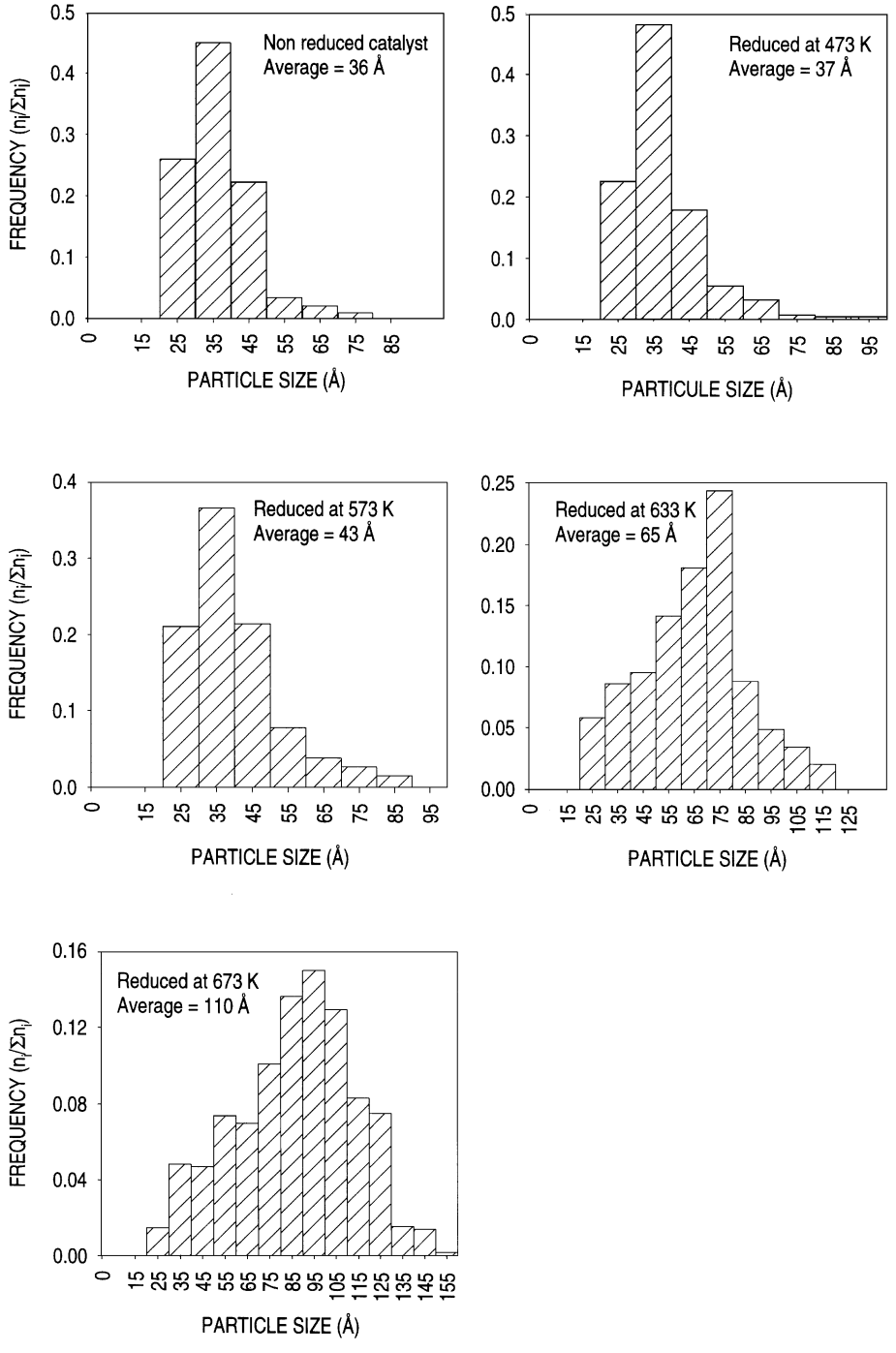

FIG. 2. HREM particle size distribution of solid reduced at various temperatures. According to XRD results (Fig. 3) the initial solid and the samples reduced at 473 and 573 K correspond to the pyrite phase while the solid reduced at 633 K is biphasic (pyrite + metal phases) and at 673 K only the metal phase is detected.

even in the presence of the gas phase suggesting that a S–H bond cleavage occurs during chemisorption. These results allow to propose a dissociative chemisorption of the thiol molecule leading to the formation of thiolate species and of a proton.

Figure 6 shows that solid-reduction does not modify the overall IR spectra of adsorbed MeSH because no new bands or shift in band position were detected but only a modification of band intensities was observed. The nonreduced solid already contains some sites able to dissociate CH_3SH. The intensity of the 2915 cm^{-1} band increases up to a reduction temperature of 473 K and then declines for higher reduction temperatures. This is better seen in Fig. 7 where the 2915 cm^{-1} band intensity was plotted as a function of

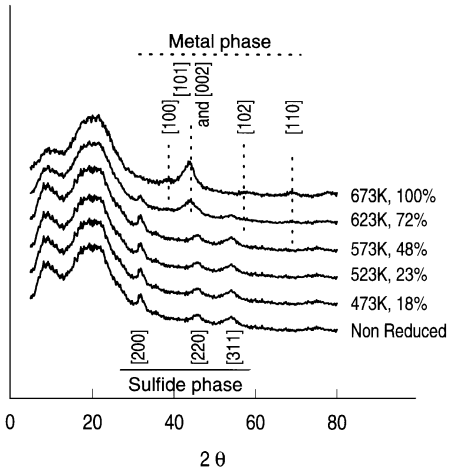

FIG. 3. XRD characterization of various reduced samples.

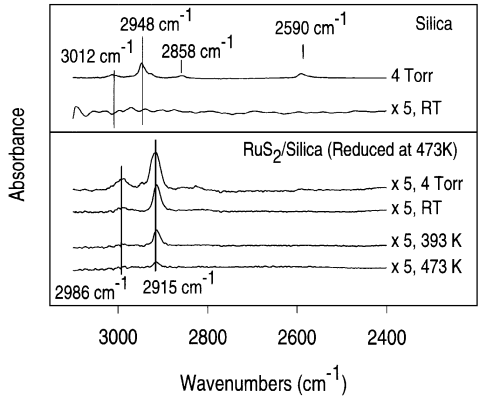

FIG. 5. IR spectra of the species resulting from CH_3SH adsorption (4 Torr at equilibrium and after evacuation at various temperatures (room temperature (RT), 393 K, 473 K)) on the silica support and on the silica-supported ruthenium sulfide reduced at 473 K.

the degree of reduction of the solid. This volcano type curve is similar to the observed variation in catalytic properties (Fig. 4) suggesting that the thiolate species is one of the intermediates involved in the disproportionation reaction. Moreover, it should be noted that the variation of band intensities goes through the same maximum irrespectively of the evacuation pretreatment suggesting that the bond strength of the CH_3S^- on the surface of the catalyst is not greatly affected by solid composition (Fig. 7).

DISCUSSION

The initial nonreduced catalyst may be considered as formed by a collection of homodispersed spherical RuS_x particles supported on the silica support. According to the total sulfur content determined either by chemical analysis or by TPR, x is close to 2.7. The presence of such a large excess of sulfur with respect to the stoichiometric RuS_2 pyrite phase was usually observed for unsupported transition metal sulfides (TMS) as well as for alumina-supported chalcogenides (42, 43). The amount of overstoichiometric sulfur species generally depends on the nature of the TMS and also on the sulfiding procedure used to convert the catalyst precursor into the corresponding sulfide phase. The nature of this species is still not completely elucidated but it does not correspond to elemental sulfur since these species resist to an evacuation at 673 K. According to Mangnus *et al.* (43) this strongly bonded sulfur species may be either overstoichiometric S_x species formed by decomposition of H_2S during the sulfidation of the solid or S–H groups and chemisorbed H_2S retained on some coordinatively unsaturated sites of the sulfided phase. However, their presence at the surface of the support itself cannot be excluded even if no H_2S can be detected during a TPR performed on the support alone because the presence of a sulfide phase may modify the adsorbing properties of silica and also may intervene as a source of spillover hydrogen which would increase the reactivity of the potential sulfur species retained

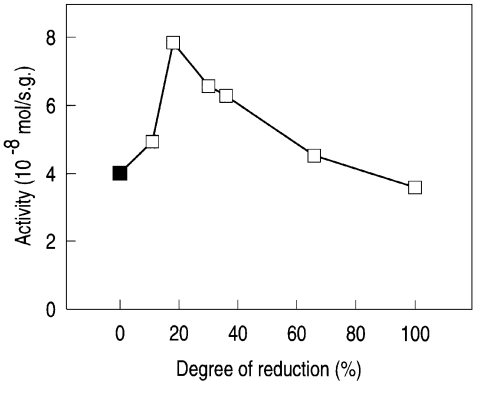

FIG. 4. Activity towards CH_3SH condensation reaction as a function of the degree of reduction of the catalyst. Reaction temperature 473 K. The black square corresponds to the activity of the nonreduced solid heated from RT to 473 K in the presence of a nitrogen flow.

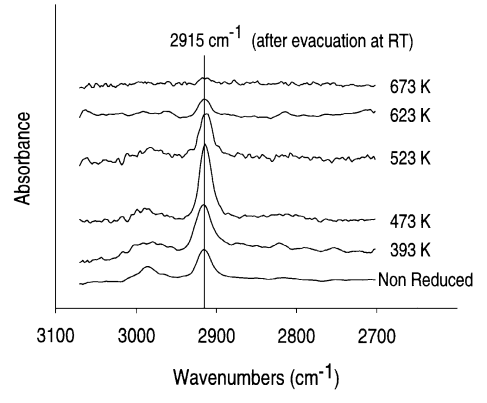

FIG. 6. IR spectra of the irreversible species resulting from CH_3SH evacuation at RT on the various reduced catalysts (the reduction temperature is given in the figure).

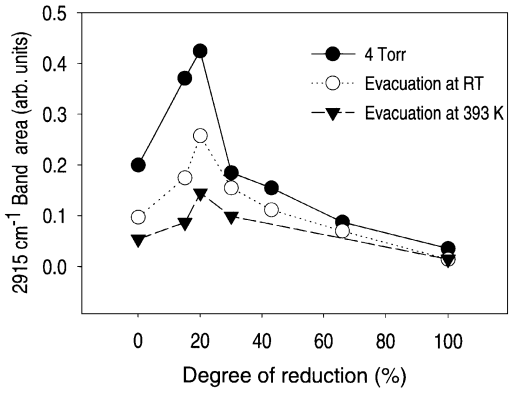

FIG. 7. Evolution of the 2915 cm^{-1} IR band area, in presence of 4 Torr of CH_3SH, and for two evacuation temperatures, versus the degree of reduction of the solid.

on the support. However, this assumption does not seem to be liable with the results presented in Fig. 5 if it is assumed that H_2S and CH_3SH interact similarly with the silica support. As a matter of fact, the bands characterizing the interaction of CH_3SH with the support do not exist on the RuS_x/SiO_2 system suggesting that the sulfided phase does not promote the adsorptive properties of the support toward sulfur-containing molecules. Therefore, the excess of sulfur appears to be more likely fixed on the ruthenium phase.

Recently, a crystallographic model representing a particle of ruthenium sulfide either unsupported or supported on alumina has been developped by Geantet *et al.* (44, 45). This model is based on a three-dimensional growth of the fcc lattice of the pyrite structure. The structure of RuS_2 can be depicted as a modified NaCl structure with two interpenetrating fcc sublattices one containing the Ru atoms and the other the S–S pairs. If n represents the number of unit cells at the edges of the growing polyhedra, the equations

$$Ru_t = 4n^3 + 6n^2 + 3n + 1 \quad [1]$$

$$S_t = 8n^3 + 12n^2 + 6n \quad [2]$$

$$S_s = 24n^2 \quad [3]$$

are established, where S represents the number of S atoms and subscripts t and s refer, respectively, to the number of ions present on the entire particle and only at the surface. In these equations the number of unit cells n is defined by

$$n = \frac{L}{\underline{a}}, \quad [4]$$

where L is the mean particle size as determined by HREM and $\underline{a}$ is the lattice parameter for RuS_2 ($\underline{a} = 5.609$ Å).

The main advantage of this model is to provide an estimation of the fraction of the different ions present at the surface of the catalyst. Taking into account the particle size distribution determined by HREM (25–45 Å), the number of ruthenium ions involved in the crystal lies between 488 and 2477. According to the model developed by Friedel in Ref. (46) for metallic particles, solids containing more than 1000 atoms exhibit the monocrystal structure while aggregates containing between 100 and 1000 ions present a transitional structure with a platonic solid shape, i.e., cubo-octahedron, icosahedron. However, if the absolute number of Ru or S ions depends on the model employed for the numbering of the different atoms, the relative amount of each species does not change in a large extent. According to this model, the sulfur to metal ratio equals 2 whatever the particle size. In such a situation, the ruthenium ions located at the corners and edges and those at the surface are sulfur deficient and may possess 3, 2, and 1 sulfur unsaturation, respectively. These CUS might be potential sites for extra sulfur accommodation and the highest conceivable S/Ru ratio might be reached when all the ruthenium ions find themselves in a sixfold coordination state. According to this model, the number of extra sulfur anions is given by

$$S_{excess} = 24n^2 + 24n + 12. \quad [5]$$

As summarized in Table 1 the S/Ru may attain 3 for a fully sulfided crystallite. This value is higher than the one determined by chemical analysis or by TPR indicating that overstoichiometric sulfur species might be linked to the sulfide phase without invoking a possible effect of the support for sulfur storage. However the nature of this extra sulfur is difficult to elucidate because the electrostatic neutrality of the crystal excludes the presence of a too high concentration of negatively charged species at its surface. Chemical analysis and TPR indicate that the composition of the nonreduced sample corresponds to $RuS_{2.7}$. This sulfur to metal ratio is lower than the one expected from the proposed model for a completely saturated crystallite. This suggests that the sulfided phase contains either some remaining Si–O–Ru links or some sulfur vacant sites. Chemical methods such as CH_3SH chemisorption evidence the presence of some vacancies because the adsorption of this molecule requires vacancy–sulfur pair.

Solid reduction indicates that the particles may be completely reduced by heating the catalysts at 673 K in the

TABLE 1

Calculated and Experimental Values of Ru_t, S_t, S_s, and S_{excess} Taking into Account an Average Particle Size of 36 Å

Species	Atoms per crystallite	Equivalent amount/g of catalyst (μmol/g)	Experimental (μmol/g)
Ru_t from [1]	1326	743	743
S_t from [2]	2650	1486 (S/Ru) = 2	
S_s from [3]	989	554	
S_{excess} [5]	1155	647	514
Total sulfur	3805	2133 (S/Ru ~ 3)	2000

presence of a hydrogen flow. For reduction temperatures lower than 573 K, the composition of the solid quickly equilibrates since H_2S is mostly formed during heating. HREM and X-ray diffraction characterizations indicated that about 45% of the total sulfur content may be removed without any significant morphological and structural modification of the particle. This amount of easily removable sulfur fits fairly well with the proposed model because it corresponds to the elimination of the amount of S_{excess} and of 50% of the calculated number of surface S–S pairs (S_s). According to the pyrite structure, the S–S pairs are orientated along the [111] directions so that one sulfur atom points out of the Ru fcc sublattice while the second one is underneath. A degree of reduction of 45% corresponds to a surface completely depleted in sulfur and to an estimated average of three vacancies per surface Ru ion assuming that at least no drastic rearrangement of the surface composition takes place during the measurements. Further sulfur removal completely overturns the system since the catalyst sinters with the concomitant formation of a metallic phase.

IR characterization of the interaction of CH_3SH with the silica support shows that the molecule does not dissociate at the surface of the support. The adsorption proceeds via hydrogen bonding with the remaining OH groups of the support. These species rapidly desorb upon evacuation at room temperature. The presence of the sulfided ruthenium phase completely modifies the nature of the chemisorbed species. The adsorption of the support strongly decreases probably because of the consumption of the OH groups during the impregnation of the support with the ruthenium salt precursor. Furthermore, the ν(S–H) band is no longer observed and the adsorbed species resist to an evacuation treatment even at temperatures as high as 473 K. This strongly suggests that this probe molecule is dissociatively adsorbed at the surface of the catalyst and its adsorption is selective on the sulfided phase. This shows that CH_3SH requires both a sulfur-deficient site to accommodate the thiolate fragment and a basic center to trap the concomitant formation of a H^+. According to these results, the nonreduced catalyst already presents a significant amount of such acid–base pairs. This is consistent with the proposed model which suggests that this solid may contain a nonnegligible amount of CUS. As evidenced in Figs. 6 and 7 the progressive reduction of the catalyst leads to noticeable changes of IR band intensities without affecting their position. This indicates that reduction does not change the nature of the adsorption but only modifies the number of adsorbing centers. Their number increases first while sulfur is removed, reaches a maximum for a degree of reduction of about 20% and then gradually diminishes when the S to metal ratio tends to 0. The variation of the number of thiolate species formed is in nice agreement with the model for the ruthenium-sulfided particle proposed above. Until a degree of reduction close to 20% (Table 1), the S_{excess} is removed inducing an increase of the number of CUS accessible to the thiolate species. For higher degrees of reduction, the amount of sulfur atoms of the lattice decreases as well as the number of basic centers required for dissociation. This points out that a degree of reduction close to 20% corresponds to a maximum of acid–base sites. Moreover, this volcano type curve correlates fairly well with the evolution of the catalytic activity with the degree of reduction indicating that the adsorbed thiolate species detected by IR spectroscopy are involved in the reaction mechanism. Taking into account the proposed model, the elimination of 20% of the initial sulfur content corresponds roughly to an average number of vacancies of about 1.5 per surface ruthenium ion. However, the model assumed that the particles are regularly shaped which should not be really the case for a particle of only 35 Å. The presence of structural defects, i.e., steps and crevices, may induce a higher concentration of superficial Ru ions. As this might lower the number of vacancies per surface ruthenium ion, it appears more likely to relate the observed maximum of chemisorption and catalytic activity to the highest concentration of Ru monovacant site–S acid–base pairs.

From either IR spectroscopy of kinetic measurements related to alcohol condensation catalyzed by oxides, it is well admitted that the first step of the reaction mechanism is the dissociative chemisorption of the reactant on an acid–base pair (47–49). This activation process leads to the formation of an alkoxide anion bonded to a surface acid site while the protonic species interacts with a basic oxygen atom of the solid leading to the formation of an OH group. This heterolytic adsorption also occurs during the interaction of thiols with the surface of oxides (36, 50).

The results of the present study show that the interaction thiol–sulfide proceeds in a similar way as the chemisorption of an alcohol with an oxidic surface. The next elemental step involves the chemisorption of a second molecule to obtain the condensation product. The SH group resulting from the dissociative adsorption of the first CH_3SH molecule could play the role of an acidic center. Indeed, current studies using dimethyl-2,6-pyridine as probe molecule, indicate that CH_3SH dissociative adsorption on sulfided CoMo catalysts, creates Brønsted acidity (51). Therefore, the second CH_3SH molecule would interact through hydrogen bonding between its sulfur atom and the proton of the surface SH group. Another possibility proposed by Padmanabhan and Eastburn for alcohols (48) is that the second activated molecule would be linked to a basic site of the surface by its hydrogen atom. This hydrogen bonding increases the electron density around the oxygen atom of that molecule favoring the nucleophilic attack of the CH_3 fragment of the alkoxide anion. Whatever the second step involved in thioether formation, it appears quite obvious that the methyl mercaptan condensation reaction requires the presence of acid–base centers to proceed.

CONCLUSIONS

Among transition metal sulfides, the pyrite MS_2 phases (Fe, Ni, Co, Ru) are known to be highly reducible because of the high reactivity of S–S pairs present on such kind of compound. These systems are therefore of great interest for basic catalytic research related to sites characterization. The study of the behavior of a model silica-supported ruthenium sulfide toward a hydrogen atmosphere has shown the possibility of preparing several reduced states without affecting the particle shape and the structure of the pyrite phase. The use of a probe molecule which dissociates at the surface of such solids is an useful tool for the identification of acid–base centers present at their surface. The IR studies of the interaction of CH_3SH with this type of solids have evidenced its dissociative chemisorption leading to a proton and a thiolate species. The concentration of the latter depends on the catalyst composition and its dependence follows the same trend as the catalytic activity, suggesting that such adsorbed species is the surface intermediate of the thioether formation. This evidences the possibility of using this test reaction to probe the acid–base properties of sulfided surfaces. With respect to spectroscopic techniques often used to characterize the interaction of probes and a solid surface, the main advantage of utilizing a reaction would be to identify the properties of solids under experimental conditions close to those used in the industrial hydrotreating applications of these sulfided materials.

ACKNOWLEDGMENTS

This work was carried out in the framework of an international program of collaboration between France and China. L.Q. thanks the "Programme de Recherches Avancées, PRA E 94-5" for financial support and G.B. gratefully acknowledges the French Ministry of Education for a Ph.D. grant.

REFERENCES

1. Topsoe, H., Clausen, B. S., and Massoth, F. E., *in* "Hydrotreating Catalysis," Catalysis Science and Technology (J. R. Anderson and M. Boudart, Eds.), Vol. 11. Springer-Verlag, Berlin/Heidelberg/New York, 1996.
2. Tanaka, K., *Adv. Catal.* **33**, 99 (1985).
3. Wambeke, A., Jaloviecki, L., Kasztelan, S., Grimblot, J., and Bonnelle, J. P., *J. Catal.* **109**, 320 (1988).
4. Jaloviecki, L., Aboulaz, A., Kasztelan, S., Grimblot, J., and Bonnelle, J. P., *J. Catal.* **120**, 108 (1989).
5. Lacroix, M., Mirodatos, C., Breysse, M., Décamp, T., and Yuan, S., *in* "Proceedings, 10th International Congress on Catalysis, Budapest, 1992" (L. Guczi, F. Solymosi, and P. Tétényi, Eds.), pp. 597–609. Akadémiai Kiadó, Budapest, 1993.
6. Joffre, J., Geneste, P., and Lerner, D. A., *J. Catal.* **97**, 543 (1986).
7. Perot, G., *Catal. Today* **10**, 447 (1991).
8. Sampson, C., Thomas, J. M., Vasudevan, S., and Wright, C. J., *Bull. Soc. Chim. Belg.* **90**, 1215 (1981).
9. Sundberg, P., Moyes, R. B., and Tomkinson, J., *Bull. Soc. Chim. Belg.* **100**, 967 (1991).
10. Wright, C. J., Fraser, D., Moyes, R. B., and Wells, P. B., *Appl. Catal.* **1**, 49 (1981).
11. Heise, W. H., Lu, K., Kuo, Y. J., Udovic, T. J., Rush, J. J., and Tatarchuk, B. J., *J. Phys. Chem.* **92**, 5184 (1988).
12. Jobic, H., Clugnet, G., Lacroix, M., Yuan, S., Mirodatos, C., and Breysse, M., *J. Am. Chem. Soc.* **115**, 3654 (1993).
13. Komatsu, T., and Hall, W. K., *J. Phys. Chem.* **95**, 9966 (1991).
14. Lacroix, M., Yuan, S., Breysse, M., Dorémieux-Morin, C., and Fraissard, J., *J. Catal.* **138**, 409 (1992).
15. Polz, J., Zeilinger, H., Müller, B., and Knözinger, H., *J. Catal.* **120**, 22 (1989).
16. Topsoe, N. Y., and Topsoe, H., *J. Catal.* **139**, 641 (1993).
17. Maternova, J., *Appl. Catal.* **6**, 61 (1982).
18. Muralidhar, G., Massoth, F. E., and Shabtai, J., *J. Catal.* **85**, 44 (1984).
19. Calais, C., Lacroix, M., Geantet, C., and Breysse, M., *J. Catal.* **144**, 160 (1993).
20. Markel, E. J., Schrader, G. L., Sauer, N. N., and Angelici, R. J., *J. Catal.* **116**, 11 (1989).
21. Portefaix, J. L., Cattenot, M., Guerriche, M., and Breysse, M., *Catal. Lett.* **9**, 127 (1991).
22. Lombardo, E., Lo Jacono, M., and Hall, W. K., *J. Catal.* **64**, 150 (1980).
23. Fierro, J. L. G., and Garcia de la Banda, J. F., *Catal. Rev. Sci. Eng.* **28**(2 & 3), 265 (1986).
24. Barthomeuf, D., *Mater. Chem. Phys.* **17**, 49 (1987).
25. Parry, E. P., *J. Catal.* **2**, 371 (1963).
26. Morterra, C., and Cerrato, G., *Langmuir* **6**, 1810 (1990).
27. Fubini, B., Giamello, E., Della Gatta, G., and Venturello, G., *J. Chem. Soc. Faraday Trans. I* **78**, 153 (1982).
28. Lavalley, J. C., Caillod, J., and Travert, J., *J. Phys. Chem.* **84**, 2080 (1980).
29. Busca, G., Rossi, P. F., Lorenzelli, V., Benaïssa, M., Travert, J., and Lavalley, J. C., *J. Phys. Chem.* **89**, 5433 (1985).
30. Santacesaria, E., Gelosa, D., Giorgi, E., and Carra, S., *J. Catal.* **90**, 1 (1984).
31. Licht, E., Schächter, Y., and Pines, H., *J. Catal.* **55**, 191 (1978).
32. Saito, Y., Cook, P. N., Niiyama, H., and Echigoya, E., *J. Catal.* **95**, 49 (1985).
33. DeCanio, E. C., Nero, V. P., and Bruno, J. W., *J. Catal.* **135**, 444 (1992).
34. Mashkina, A. V., Grunvald, V. R., Nasteka, V. I., Borodin, B. P., Yakovleva, V. N., and Khairulina, L. N., *React. Kinet. Catal. Lett.* **41**, 357 (1990).
35. Pecoraro, T. A., and Chianelli, R. R., *J. Catal.* **67**, 430 (1981).
36. Lacroix, M., Boutarfa, N., Guillard, C., Vrinat, M., and Breysse, M., *J. Catal.* **120**, 473 (1989).
37. Knop, O., *Can. J. Chem.* **41**, 1838 (1963).
38. Huntley, D. R., *J. Phys. Chem.* **93**, 6156 (1989).
39. Huntley, D. R., *J. Phys. Chem.* **99**, 12907 (1995).
40. Saur, O., Chevreau, T., Lamotte, J., Travert, J., and Lavalley, J. C., *J. Chem. Soc. Faraday Trans. I* **77**, 427 (1981).
41. Lavalley, J. C., *Catal. Today* **27**, 377 (1996).
42. Lacroix, M., Boutarfa, N., Guillard, C., Vrinat, M., and Breysse, M., *J. Catal.* **120**, 473 (1989).
43. Mangnus, P. J., Riezebos, A., van Langeveld, A. D., and Moulijn, J. A., *J. Catal.* **151**, 178 (1995).
44. Geantet, C., Calais, C., and Lacroix, M., *Compt. Rend. Acad. Sci. Fr.* **315**(II), 439 (1992).
45. De los Reyes, Vrinat, M., Geantet, C., and Breysse, M., *Catal. Today* **10**, 645 (1991).
46. Joyes, P., *in* "Les agrégats inorganiques élémentaires," les Editions de Physique, Paris, 1990.
47. Figueras, F., Nohl, A., de Mourques, L., and Trambouze, Y., *Trans. Faraday Soc.* **67**, 1155 (1971).
48. Padmanabhan, V. R., and Eastburn, F. J., *J. Catal.* **24**, 88 (1972).
49. Knözinger, H., Bühl, H., and Ress, E., *J. Catal.* **12**, 121 (1968).
50. Sugioka, M., Kamanaka, T., and Aomura, K., *J. Catal.* **52**, 531 (1978).
51. Petit, C., Maugé, F., and Lavalley, J. C., *Stud. Surf. Sci.* **106**, 157 (1997).